

Matrix Isolation and Transient Photochemistry of Ru(dmpe)₂H₂: Characterization and Reactivity of Ru(dmpe)₂ (dmpe = Me₂PCH₂CH₂PMe₂)

Chris Hall,^{1a} William D. Jones,^{*,1b} Roger J. Mawby,^{1a} Robert Osman,^{1a}
Robin N. Perutz,^{*,1a} and Michael K. Whittlesey^{1a}

Contribution from the Department of Chemistry, University of York, York YO1 5DD, U.K., and Department of Chemistry, University of Rochester, Rochester, New York 14627.

Received March 24, 1992

Abstract: The photochemistry of *cis*-Ru(dmpe)₂H₂ (dmpe = Me₂PCH₂CH₂PMe₂) has been studied by IR and UV/vis spectroscopy in methane, argon, and CO-doped argon matrices, by UV/vis spectroscopy following laser flash photolysis in solution, and by IR and NMR methods following steady-state irradiation. The UV photolysis of Ru(dmpe)₂H₂ in methane and argon matrices generates Ru(dmpe)₂ in two forms exhibiting similar three-band UV/vis spectra. The forms are distinguished by selective photolysis into their visible bands: one regenerates the precursor, while the other gives an unidentified product. Photolysis in CO-doped argon matrices generates Ru(dmpe)₂CO. Pulsed laser photolysis (308 nm) of Ru(dmpe)₂H₂ allows the generation of Ru(dmpe)₂ in solution at 300 K. In the absence of added ligands it decays by reaction with expelled dihydrogen, regenerating the starting material (second-order kinetics). In the presence of other ligands, Ru(dmpe)₂ reacts by pseudo-first-order kinetics with second-order rate constants decreasing in the order H₂ ≈ CO > Me₃CNC > PMe₃ > C₂H₄ ≈ Et₃SiH > cyclopentene. The rate constants for the reactions with H₂ and CO are close to the diffusion limit. The enthalpies of activation for reaction with Et₃SiH and Me₃CNC are 8.9 ± 1.1 and 2.3 ± 0.6 kJ mol⁻¹, respectively. The steady-state photolysis of Ru(dmpe)₂H₂ gives rise to the following products: Ru(dmpe)₂CO with CO, *cis*-Ru(dmpe)₂(SiEt₃)H with Et₃SiH, *cis*-Ru(dmpe)₂(C₂H₃)H and Ru(dmpe)₂(C₂H₄) with C₂H₄, and *cis*-Ru(dmpe)₂(CN)₂ with Me₃CNC. The rapid reaction of Ru(dmpe)₂ with H₂ limits the application of Ru(dmpe)₂H₂ as a precursor for C-H activation reactions. The combination of rapid reaction kinetics with very low-energy visible absorption maxima is best explained if Ru(dmpe)₂ has a singlet ground state with a square-planar coordination geometry.

Introduction

The discovery by Chatt and Davidson in 1965 that *trans*-Ru(dmpe)₂Cl₂ (dmpe = bis(dimethylphosphino)ethane) reacts with arene radical anions to yield the aryl hydride complexes Ru(dmpe)₂(aryl)H represented the first evidence for intermolecular C-H activation of an arene by a transition-metal complex.² These authors proposed Ru(dmpe)₂ as an intermediate in this reaction, but only the dimer [Ru(dmpe)(μ-Me₂PCH₂CH₂PMeCH₂)H]₂ has been characterized.³ The arene activation reactions were examined in more detail by Ittel et al., who showed that the (naphthyl)hydride complex was converted to the corresponding (phenyl)hydride complex on heating in benzene.⁴

The dihydride complex Ru(dmpe)₂H₂ was first reported² in 1965 and characterized more thoroughly by Tolman et al., who showed that *cis*-Ru(dmpe)₂H₂ is formed by heating Ru(dmpe)₂(C₁₀H₇)H under 1 atm of H₂ at 65 °C.⁵ Later, Jones and Kosar used Ru(dmpe)₂H₂ as an alternative source of Ru(dmpe)₂ in their catalytic synthesis of indoles.⁶ The dihydride complex was proposed to undergo concerted loss of H₂ upon photolysis to give the 16-electron intermediate. At about the same time, Bergamini et al. demonstrated that photoinduced loss of H₂ from Ru(dmpe)₂H₂ is indeed concerted.⁷ The product of photolysis (λ = 313 nm) of the dihydride complex in toluene at room temperature in the absence of other ligands was identified as the dimer, Ru₂(dmpe)₅. Photolysis in benzene solution in the presence of added C₂H₄ led to the formation of Ru(dmpe)₂(C₂H₄),⁷ although the product was incompletely characterized.

Field and co-workers have addressed the problem of C-H activation reactions with Ru(dmpe)₂H₂.⁸ Room-temperature

photolysis (λ > 285 nm) in benzene results in the formation of the phenyl hydride complex, *cis*-Ru(dmpe)₂(C₆H₅)H, in 40% yield after 9.5 h, i.e., far more slowly than the corresponding reaction of Fe(dmpe)₂H₂.⁹ In contrast to the results of Bergamini et al., irradiation in toluene solution at room temperature afforded a mixture of one *trans* and two *cis* (aryl)hydride products. Photolysis of Ru(dmpe)₂H₂ at room temperature in neat cyclopentene (λ > 285 nm) generated a mixture of the cyclopentenyl hydride complex, *cis*-Ru(dmpe)₂(C₅H₇)H, and two *trans* products but no η²-alkene complex as shown by ¹H and ³¹P NMR spectroscopy. Photolysis at room temperature in alkane solvents (pentane, hexane, or heptane) failed to effect alkane C-H activation or other reactions. Many more examples of C-H activation by related metal phosphine complexes of the iron group have been found.^{4,9-14}

The circumstantial evidence strongly implicates photochemical reductive elimination from Ru(dmpe)₂H₂ to form the coordinatively unsaturated 16-electron Ru(0) intermediate, Ru(dmpe)₂. Mononuclear complexes of Ru(0) which are 4-coordinate are very rare indeed; the best established example is Ru(η²-styrene)₂(PPh₃)₂.¹⁵ Ruthenium tetracarbonyl has been shown by time-resolved infrared spectroscopy in the gas phase to have a singlet

(8) Yau, B.; Field, L. D. Personal communication.

(9) Baker, M. V.; Field, L. D. *J. Am. Chem. Soc.* **1986**, *108*, 7433.

(10) Werner, H.; Werner, R. *J. Organomet. Chem.* **1981**, *209*, C60.

Hartwig, J. F.; Andersen, R. A.; Bergman, R. G. *Organometallics* **1991**, *10*,

1710. Koola, J. D.; Roddick, D. M. *J. Am. Chem. Soc.* **1991**, *113*, 1450.

(11) Werner, H.; Werner, R. *Angew. Chem., Int. Ed. Engl.* **1981**, *20*, 793.

(12) Desrosiers, P. J.; Shinomoto, R. S.; Flood, T. C. *J. Am. Chem. Soc.*

1986, *108*, 1346, 7964. Harper, T. G. P.; Shinomoto, R. S.; Deming, M. A.;

Flood, T. C. *J. Am. Chem. Soc.* **1988**, *110*, 7915. Shinomoto, R. S.; Desrosiers,

P. J.; Harper, T. G. P.; Flood, T. C. *J. Am. Chem. Soc.* **1990**, *112*, 5047.

Ermer, S. P.; Shinomoto, R. S.; Deming, M. A.; Flood, T. C. *Organometallics*

1989, *8*, 1377.

(13) Jones, W. D.; Foster, G. P.; Putinas, J. M. *J. Am. Chem. Soc.* **1987**,

109, 5047.

(14) Antberg, M.; Dahlenburg, L. *Angew. Chem., Int. Ed. Engl.* **1986**, *25*,

260; *J. Organomet. Chem.* **1986**, *312*, C67. Dahlenburg, L.; Frosin, K.-M.

Chem. Ber. **1988**, *121*, 865.

(15) De C. T. Carrondo, M. A. A. F.; Chaudret, B. N.; Cole-Hamilton,

D. J.; Skapski, A. C.; Wilkinson, G. *J. Chem. Soc., Chem. Commun.* **1978**,

463. Chaudret, B. N.; Cole-Hamilton, D. J.; Wilkinson, G. *J. Chem. Soc.,*

Dalton Trans. **1978**, 1739.

(1) (a) University of York. (b) University of Rochester.

(2) Chatt, J.; Davidson, J. M. *J. Chem. Soc.* **1965**, 843.

(3) Cotton, F. A.; Hunter, D. L.; Frenz, B. A. *Inorg. Chim. Acta* **1975**,

15, 155.

(4) Ittel, S. D.; Tolman, C. A.; English, A. D.; Jesson, J. P. *J. Am. Chem.*

Soc. **1976**, *98*, 6073.

(5) Tolman, C. A.; Ittel, S. D.; English, A. D.; Jesson, J. P. *J. Am. Chem.*

Soc. **1978**, *100*, 4080.

(6) Jones, W. D.; Kosar, W. P. *J. Am. Chem. Soc.* **1986**, *108*, 5640.

(7) Bergamini, P.; Sostero, S.; Traverso, O. *J. Organomet. Chem.* **1986**,

299, C11.

Table I. IR Bands of Ru(dmpe)₂H₂ in Matrices at 12 K^a ($\bar{\nu}$ /cm⁻¹)

argon		methane		argon		methane	
2969 m	c	$\nu(\text{CH})$		936 s	937 m		
2913 m	2900			930 s	931 m	$\rho(\text{CH}_3)$	
1783 m ^b	1809			924 s	925 s		
1779 m	1800 m			884 s	886 s		
1775 m	1792 m	$\nu(\text{RuH})$		829 m	830 s		
1767 m	1785 m ^b			787 m	nr		
1765 m	1723 m			708 m	nr		
1418 m	1419 m			697 m	nr		
1288 m	c			640 s	nr		
1273 m	c						

^a Only the medium and strong bands are listed. nr = not recorded.

^b Most intense of $\nu(\text{RuH})$ modes. ^c Obscured by methane absorptions.

ground state,^{16a} but its geometry could not be determined. Ab initio calculations on Ru(CO)₄ suggest that the ground state is a singlet with a C_{2v} geometry.^{16b}

In this paper we employ the photolysis of Ru(dmpe)₂H₂ to generate monomeric Ru(dmpe)₂. Its UV/vis spectrum in low-temperature matrices (Ar, CH₄) proves highly characteristic, while its reactivity toward CO can be followed by IR spectroscopy. The spectra and reaction kinetics of Ru(dmpe)₂ in solution prove amenable to study by laser flash photolysis with UV/vis detection: it is indeed highly reactive, combining with hydrogen and CO at a rate close to diffusion-controlled and with other substrates somewhat more slowly.

Results

1. Matrix Photochemistry of Ru(dmpe)₂H₂. a. Photolysis in Methane and Argon Matrices. Ru(dmpe)₂H₂ is a white compound which sublimates at a convenient rate for matrix isolation when heated to 60–70 °C. The matrix UV spectrum shows a steadily increasing absorption from 300 to 200 nm with a slight shoulder at ca. 250 nm.

We consider the effect of photolysis of Ru(dmpe)₂H₂ in methane first of all since we have the most extensive information for this matrix. The infrared spectrum (Figure 1a(i), Table I) of Ru(dmpe)₂H₂ isolated in a methane matrix at 12 K exhibits a group of metal hydride stretching bands with many overlapping components, the most intense at 1785 cm⁻¹ (cf. 1775 cm⁻¹ in toluene solution).⁷ The spectrum in other regions is much sharper and relatively free of matrix splittings. Such behavior is typical of metal hydride complexes.¹⁷ Irradiation of Ru(dmpe)₂H₂ isolated in a methane matrix for 60 min (Xe arc filtered to 234–376 nm) effected ca. 40% reduction of the $\nu(\text{RuH})$ bands of the starting material (Figure 1a(ii)). No new $\nu(\text{RuH})$ modes were observed to grow in, but there were slight alterations in the relative intensities of the component bands. The only distinct product band elsewhere in the IR spectrum was a weak feature at 1204 cm⁻¹, although interactive subtraction indicated the presence of product bands overlapping with those of the precursor in the regions of intense dmpe bands.¹⁸ In contrast, the visible part of the spectrum showed the appearance of new bands at 366 (sh), 448, 531, 610 (sh), and 732 nm (Figure 2a(I)). We have employed selective photolysis to test whether all bands derive from one product.

Subsequent long-wavelength irradiation (490–509 nm, 20 min) designed to select the blue side of the central band reduced the intensity of all of the visible bands by about 30% and caused a recovery in the IR bands of the starting material of only ca. 6% (Figure 1a(iii)). No new bands were observed in the IR spectrum. At the same time, the maximum of the central visible band shifted to the red, so it now appeared at 537 nm (Figure 2a(II)). Subtraction of the spectrum after selective photolysis from that beforehand showed maximum depletion at 444, 511, and 736 nm

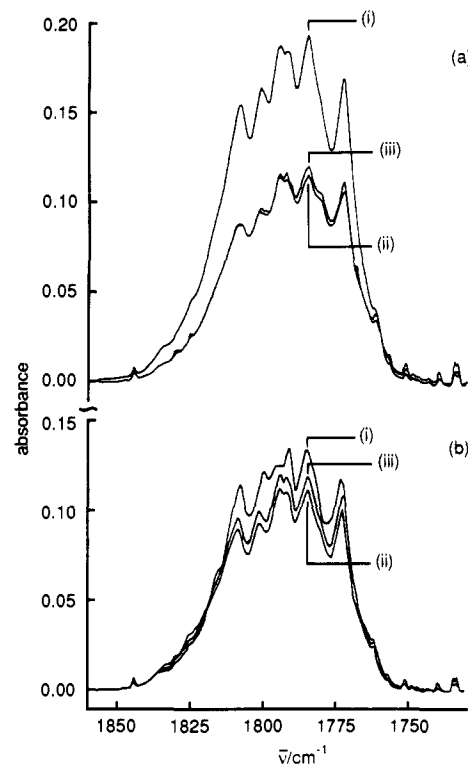


Figure 1. IR spectra of Ru(dmpe)₂H₂ in methane matrix at 12 K in the metal hydride stretching region. (Note that the UV/vis spectra from the same experiments appear in Figure 2.) (a) Spectra (i) after 150 min of deposition, (ii) after 60 min of UV irradiation with Xe arc (234–376 nm), and (iii) after 20 min of subsequent selective photolysis (490–509 nm). (b) Spectra from a separate experiment (i) after deposition, (ii) after 45 min of UV irradiation (234–376 nm), and (iii) after 30 min of subsequent selective irradiation (540–600 nm).

Table II. UV/Vis Band Maxima (nm) for Photoproducts of *cis*-Ru(dmpe)₂H₂ from Difference Spectra in Matrices

after initial photolysis ^a	after photolysis in short wavelength tail ^b		after photolysis in long wavelength tail ^c	
	depletion maximum	residual maximum	depletion maximum	residual maximum
Argon Matrix				
365 sh				
460	456	460	463	458
543	535	554	559	531
666 sh				
743	743	744	747	741
Methane Matrix				
ca. 366 sh				
448	444	452	451	449
531	511	537	543	526
ca. 610 sh				
732	736	727	734	716

^a Photolysis wavelength 234–376 nm. ^b Photolysis wavelengths: argon $\lambda = 510$ –530 nm, methane $\lambda = 490$ –509 nm. Range quoted for absorbance of filter <1.0. ^c Photolysis wavelengths: argon $\lambda = 575$ –595 nm, methane $\lambda = 540$ –600 nm.

(Figure 2a(III), Table II). A similar experiment was performed in which initial generation of product (Figures 1b(i), (ii) and 2b(I)) was followed by selective photolysis between 540 and 600 nm (30 min) on the red side of the central maximum. The selective photolysis caused a 33% decrease in the intensities of the visible bands (Figure 2b(II)) and an almost identical recovery (32% in the intensities of the IR bands of the precursor (Figure 1b(iii)). There was again a significant shift of the central visible band (now at 526 nm), but in the opposite direction to that observed previously. The depletion maxima were now at 451, 543, and 734 nm (Figure 2b(III)). In addition to the striking shifts of the central band, there are smaller but reproducible shifts in the band at ca.

(16) (a) Bogdon, P. L.; Weitz, E. *J. Am. Chem. Soc.* **1989**, *111*, 3163. (b) Ziegler, T.; Tschinke, V.; Fan, L.; Becke, A. D. *J. Am. Chem. Soc.* **1989**, *111*, 9177.

(17) Girling, R. B.; Grebenik, P.; Perutz, R. N. *Inorg. Chem.* **1986**, *25*, 31.

(18) Bands of the photoproduct detected by interactive subtraction of the starting spectrum: (i) in methane matrices 937, 931, 927, 895, 886, 877 cm⁻¹; (ii) in argon matrices 1422, 1288, 1274, 936, 925, 923, 885, 828 cm⁻¹.

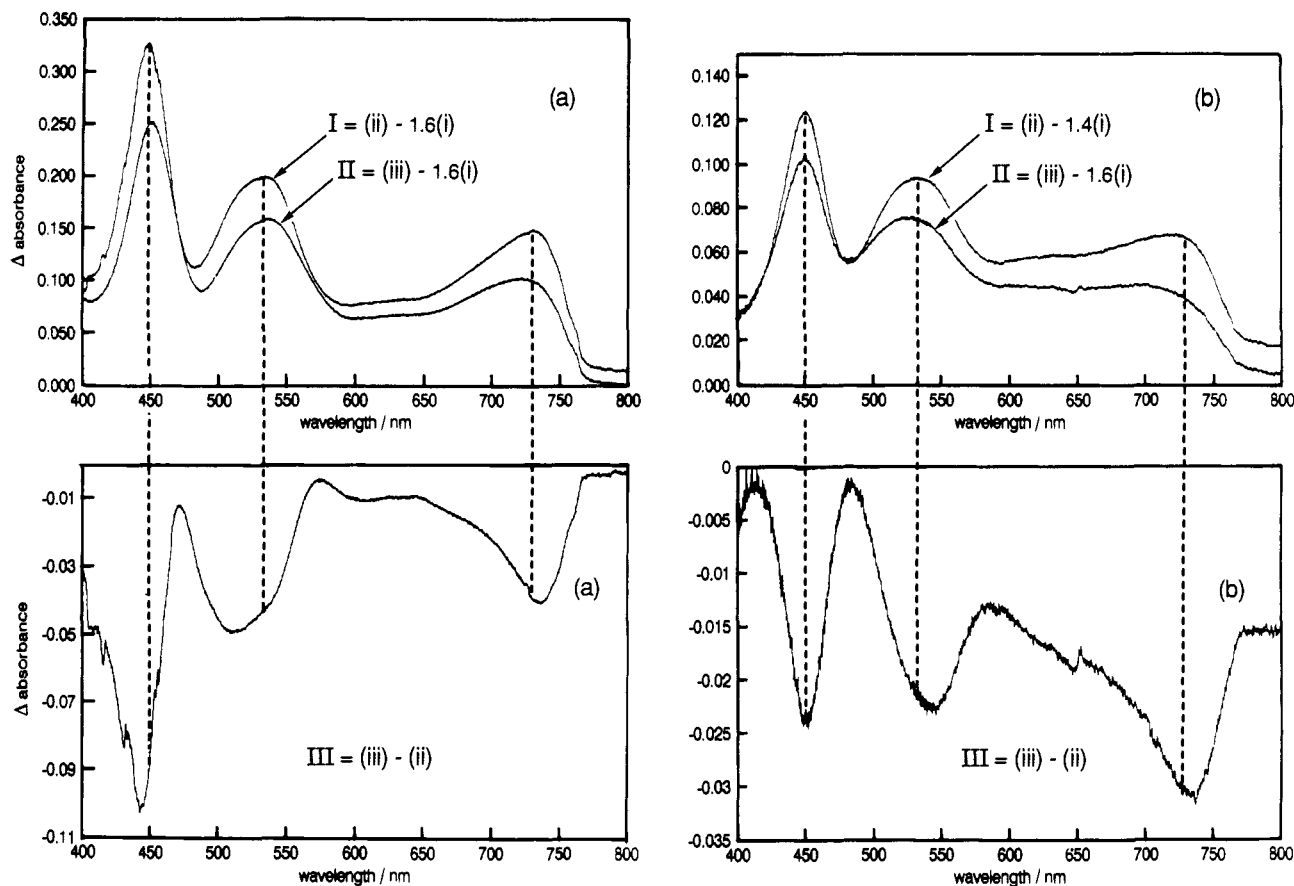


Figure 2. UV/vis difference spectra following photolysis of $\text{Ru}(\text{dmpe})_2\text{H}_2$ in methane matrix recorded in the same two experiments as the IR spectra of Figure 1 and labeled correspondingly. The deposition spectrum, i, not illustrated, was simply a scatter curve. The top spectra are obtained by subtraction of a multiple of the deposition spectrum in order to remove the effects of scatter.

450 nm (Table II). The shifts in the third band at ca. 730 nm are harder to discern since the band is very diffuse.

We conclude that there are probably two species, P_{irrev} and P_{rev} , contributing to each band with similar, but not identical, band maxima and extinction coefficients. Product P_{rev} , with visible bands to longer wavelength, reacts on selective irradiation to reform $\text{Ru}(\text{dmpe})_2\text{H}_2$. Selective irradiation of P_{irrev} , the product with the shorter wavelength set of maxima, generates another unidentified photoproduct with no $\nu(\text{RuH})$ bands. Estimates of the absorption maxima of the two species contributing to the spectra can be obtained from the depletion spectra after selective photolysis. Similar estimates were obtained from the spectra of the material remaining after selective photolysis (labeled residual maxima in Table II).

Photolysis of $\text{Ru}(\text{dmpe})_2\text{D}_2$ in a methane matrix provides a test for methane activation since there should be little interference from bands in the $\nu(\text{RuH})$ region in the precursor spectrum. A sample of $\text{Ru}(\text{dmpe})_2\text{D}_{2-x}\text{H}_x$ (82% deuterated) isolated in methane exhibited a $\nu(\text{RuH})$ band at 1785 cm^{-1} with absorbance 0.05, due to the residual hydride. However, after 120 min of irradiation ($\lambda > 200\text{ nm}$), no IR product bands were detected in the metal hydride stretching region, but two new bands were observed at 894 and 876 cm^{-1} . The presence of three product bands at 450 , 533 , and 730 nm in the visible spectrum confirms that the same product was generated as in previous experiments.

The infrared spectrum of $\text{Ru}(\text{dmpe})_2\text{H}_2$ in an argon matrix exhibits a group of metal hydride stretching bands with a splitting pattern different from that observed in methane (Table I). Irradiation at $\lambda > 285\text{ nm}$ had a negligible effect on the spectrum. Shorter wavelength irradiation (Xe arc, $234\text{--}376\text{ nm}$, 60 min) reduced the absorbance of the hydride bands of the starting material by 23%. No new Ru-H stretching bands were observed to grow in, but there was some redistribution of intensity among the components of the $\nu(\text{RuH})$ bands of $\text{Ru}(\text{dmpe})_2\text{H}_2$. The only distinct product band observed by IR spectroscopy was a weak

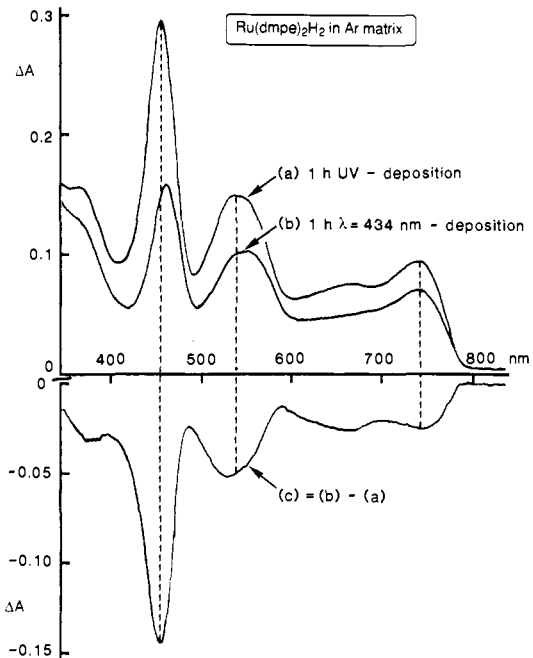


Figure 3. UV/vis difference spectra following photolysis of $\text{Ru}(\text{dmpe})_2\text{H}_2$ in argon matrix: (a) spectrum following 60 min of UV photolysis ($234\text{--}376\text{ nm}$) minus (deposition spectrum); (b) spectrum following subsequent 60 min of selective photolysis ($426\text{--}445\text{ nm}$) minus (deposition spectrum); (c) spectrum obtained by subtraction of spectrum a from spectrum b showing shift in the central maximum.

feature at 1303 cm^{-1} (obscured by bands of the matrix in the methane experiments), but further bands were revealed by interactive subtraction.¹⁸ In the UV/vis spectrum, new bands grow at 365 (sh), 460 , 543 , 666 (sh), and 743 nm (Figure 3a). As

Table III. UV/Vis Band Maxima and Assignments for Ru(dmpe)₂, Comparison of Matrix^a and Solution Species, λ/nm (ε/dm³ mol⁻¹ cm⁻¹)^b

argon matrix		methane matrix		solution			assignment
P _{irrev}	P _{rev}	P _{irrev}	P _{rev}	cyclohexane	pentane		
456	463	444	451	467 (2400) ^c	468	d _{z²} → p _{x,y}	
535	559	511	543	555 (1700) ^c	548	d _{xz,yz} → p _z	
743	747	736	734	745 (1900) ^c	724	d _{z²} → p _z	

^a The matrix spectra also show shoulders at 365 (Ar and methane), 666 (argon only), 610 nm (methane only). ^b Error bars ±5 nm for absolute wavelength. ^c Estimated from the kinetics in the absence of added H₂ and from the relative intensities of the bands.

in methane matrices, we have examined the effect of selective photolysis. On irradiation with 426–443 nm (60 min) corresponding to the short wavelength side of the most intense band, all product bands were depleted, but the proportion removed varied from ca. 50% for the most intense band to ca. 25% for the 740-nm band. The IR spectrum showed a recovery of only ca. 4% in the ν(RuH) bands of the precursor with a slight alteration in the relative intensities of the components. The selective photolysis caused a notable shift of two of the UV/vis band maxima to longer wavelengths: the band at 459 nm shifted 5 nm and that at 541 nm shifted 11 nm (Figure 3b). Subtraction spectra showed maximum depletion at 455, 532, and 747 nm. Finally, photolysis with λ > 400 nm (20 min) bleached the product bands completely. This type of experiment was repeated with selective photolysis on either side of the central band (λ = 510–530 and 575–595 nm) with results similar to those observed in methane matrices (Table II).

The effect of increasing the matrix dilution of an argon matrix was tested by subliming the Ru(dmpe)₂H₂ at a temperature of 56 °C, 9 °C lower than normal. The matrix IR bands of the precursor were reduced in intensity by a factor of 4.3 for the same deposition time, but the UV/vis product bands were observed at 459, 543, and 755 nm, close to their previous positions. Selective photolysis with λ = 432–440 nm shifted the central maximum to 565 nm, confirming that both species P_{irrev} and P_{rev} were present. No recovery in the IR bands was observed. The experiments described above were designed for selectivity, rather than for maximum conversion. In a separate experiment also under dilute conditions, the sample was irradiated with a water-filtered mercury arc (λ > 200 nm), leading to 80% reduction of ν(RuH) modes after 60 min of photolysis.

The data allow comparison of the band maxima in the UV/vis spectra of each component, P_{rev} and P_{irrev}, of the product in argon with those in methane (Table III). The red shifts from argon to methane matrices are modest, varying between 200 and 670 cm⁻¹. Alternatively, P_{irrev} and P_{rev} may be compared with one another. The shifts between P_{irrev} and P_{rev} are ca. 300 cm⁻¹ on the shortest wavelength band, ca. 800 cm⁻¹ on the central band, and ca. 70 cm⁻¹ on the longest wavelength band. The band maxima of the reversible product, P_{rev}, always lie to the long wavelength side of the irreversible product, P_{irrev}.

b. Photolysis in CO-Doped Argon Matrices. Irradiation (λ > 285 nm) of Ru(dmpe)₂D_{2-x}H_x isolated in a 1.5% CO/Ar matrix for 6 min led to the formation of a new band at 1859 cm⁻¹, which may be readily assigned to ν(CO) of Ru(dmpe)₂(CO) (Figure 4).¹⁹ On prolonged photolysis other new bands appear from secondary reactions, first at 1929 and then at 1909 cm⁻¹; these grow independently of one another.

c. Assignment of Matrix Photoproducts. The matrix isolation experiments show that the photoproducts in argon or methane have three conspicuous bands in the visible region. The effect of dilution and the sharp IR bands outside the ν(RuH) region indicate that the products are mononuclear. The infrared evidence argues for the absence of hydride groups in the products, but it

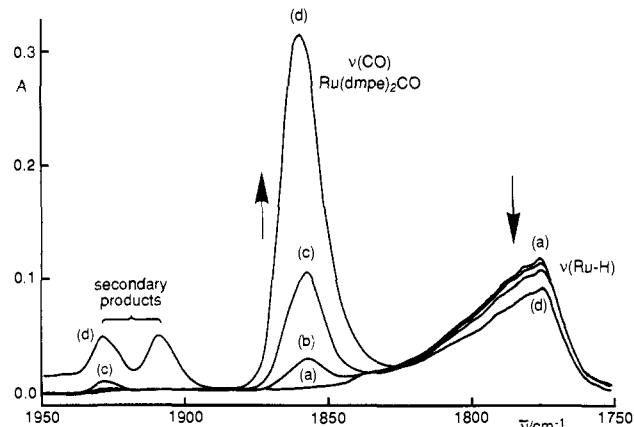


Figure 4. IR spectra of Ru(dmpe)₂D_{2-x}H_x (82% D) in argon matrix doped with 1.5% CO in the ν(CO) region: (a) after deposition (note the band at ca. 1780 cm⁻¹ due to residual hydride in the sample); (b) after 1 min of photolysis; (c) after 5 min more photolysis; (d) after 25 min more photolysis (λ > 285 nm).

does not give positive evidence of their identity. There is no evidence for reaction with methane or coordination by methane. Selective photolysis reveals that there are two contributors, P_{rev} and P_{irrev}, to the UV/vis spectrum. They have slightly different band maxima and extinction coefficients but the same pattern of bands, suggesting that the same molecule is present in two different environments (Table III). Long wavelength photolysis converts P_{rev} back to Ru(dmpe)₂H₂, a common characteristic of coordinatively unsaturated organometallics in matrices.²⁰ On the other hand, P_{irrev} is converted to another unidentified product on long wavelength irradiation. If CO is introduced into the matrix, the first observed product is Ru(dmpe)₂CO.

All of the evidence is consistent with an identification of the primary product in argon and methane matrices as Ru(dmpe)₂ formed in two environments (see Discussion); strong support for this assignment comes from the flash photolysis experiments described below.

2. Laser Flash Photolysis Studies of Ru(dmpe)₂H₂. Ru(dmpe)₂H₂ exhibits an absorption maximum at 210 nm in pentane solution (ε = 4900 dm³ mol⁻¹ cm⁻¹) and a shoulder at 260 nm. The extinction coefficient at 308 nm (the laser wavelength) is 170 dm³ mol⁻¹ cm⁻¹.⁸

a. Laser Flash Photolysis without Quenchers. Laser flash photolysis (laser wavelength 308 nm, pulse width ca. 5 ns) of Ru(dmpe)₂H₂ in cyclohexane (ca. 4 × 10⁻³ mol dm⁻³) under argon resulted in the rapid formation of a transient species which absorbed strongly at 467, 555, and 745 nm (Figure 5b, cf. matrix spectrum in Figure 5a). The rise time of the transient is governed by the instrument response, i.e., rise time < 30 ns. The transient decayed with second-order kinetics, returning to the base line over hundreds of microseconds (k₂/εl = 2.8 × 10⁶ s⁻¹, monitored at 470 nm) (Figure 6a). The rate of decay was the same irrespective of which band maximum was used as the monitoring wavelength. On changing the alkane solvent from cyclohexane to pentane, the same transient was observed with bands at 468, 548, and 724 nm. The decay was again second order returning to the base line (k₂/εl = 1.9 × 10⁶ s⁻¹). The UV/vis spectra of solutions in either cyclohexane or pentane were found to be unchanged after 200 laser shots. When the experiment was repeated in pentane solution under an atmosphere of methane rather than argon, the rate of decay of the transient was unaltered.

Two types of experiments were conducted in order to examine the effect of concentration of Ru(dmpe)₂H₂ on the kinetics. In the first, the concentration of Ru(dmpe)₂H₂ was increased by a factor of 2 at constant path length, resulting in a 6% reduction in the value of k₂/εl. This change is within the error limits of the experiment. In the second, the concentration of Ru(dmpe)₂H₂

(19) Jones, W. D.; Libertini, E. *Inorg. Chem.* **1986**, *25*, 1794. The value of ν(CO) for Ru(dmpe)₂CO is quoted incorrectly in this paper. It should be 1845 (s) and 1825 (sh) cm⁻¹ rather than 1945 and 1925 cm⁻¹.

(20) Hitam, R. B.; Mahmoud, K. A.; Rest, A. J. *Coord. Chem. Rev.* **1984**, *55*, 1.

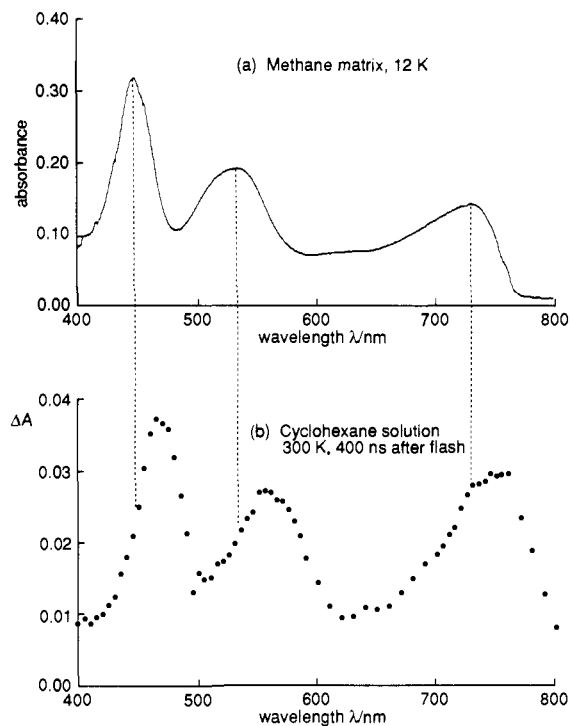


Figure 5. (a) Spectrum obtained following photolysis of $\text{Ru}(\text{dmpe})_2\text{H}_2$ in methane matrix at 12 K. (b) Transient UV/vis spectrum obtained 400 ns after laser flash photolysis (308 nm) of $\text{Ru}(\text{dmpe})_2\text{H}_2$ in cyclohexane solution at 300 K.

was increased by a factor of 5, and the path length of the cuvette decreased by a corresponding factor. The decay was more rapid, no longer fitted simple second-order (or first-order) kinetics, and did not return to the base line, implying that bimolecular processes set in at high concentrations (ca. $2 \times 10^{-2} \text{ mol dm}^{-3}$).

A change of the solvent to benzene was found to have no significant effect on the position of the bands for the transient nor on its rate of decay compared to cyclohexane. Again, the UV/vis spectrum of the sample was found to be unchanged after 200 laser shots.

b. Quenching by Hydrogen. Laser flash photolysis of $\text{Ru}(\text{dmpe})_2\text{H}_2$ in cyclohexane was carried out under varying pressures of H_2 (always made up to a total pressure of 1 atm with argon). The presence of hydrogen caused an increase in the rate of decay of the transient monitored at 470 nm (Figure 6b). The transient was found to decay with pseudo-first-order kinetics, and a plot of k_{obsd} versus $p[\text{H}_2]$ is linear. With the solubility²¹ of H_2 taken as $3.8 \times 10^{-3} \text{ mol dm}^{-3} \text{ atm}^{-1}$, a value is obtained for the second-order rate constant for the reaction with hydrogen of $(6.8 \pm 0.3) \times 10^9 \text{ dm}^3 \text{ mol}^{-1} \text{ s}^{-1}$ (Figure 7a). Under 1 atm of H_2 , the lifetime (k^{-1}) of the transient is calculated to be 39 ns, which is too rapid to be observed on our equipment.

Laser flash photolysis of $\text{Ru}(\text{dmpe})_2\text{D}_2$ under a deuterium atmosphere was examined in order to determine the kinetic isotope effect on this reaction. A sample of $\text{Ru}(\text{dmpe})_2\text{D}_2$ in cyclohexane under 50 Torr of $\text{D}_2/700$ Torr of argon was investigated side-by-side with a sample of dihydride under an identical pressure of H_2/argon . The observed rate constant, k_{obsd} , for the reaction with H_2 is $2.06 \times 10^6 \text{ s}^{-1}$ compared to $1.71 \times 10^6 \text{ s}^{-1}$ for the reaction with deuterium. The estimated error in the measurements is $\pm 5\%$, which leads to a value of $k_{\text{H}}/k_{\text{D}} = 1.20 \pm 0.08$. The experiment was repeated at a lower pressure of quenching gas (9 Torr of H_2 or D_2), giving rates of 4.90×10^5 and $3.64 \times 10^5 \text{ s}^{-1}$ for hydrogen and deuterium, respectively, and a value of $k_{\text{H}}/k_{\text{D}} = 1.35 \pm 0.1$.

c. Quenching by Carbon Monoxide and Ethene. Laser flash photolysis in cyclohexane under varying pressures of CO (pressure made up to 1 atm with argon) again led to quenching of the

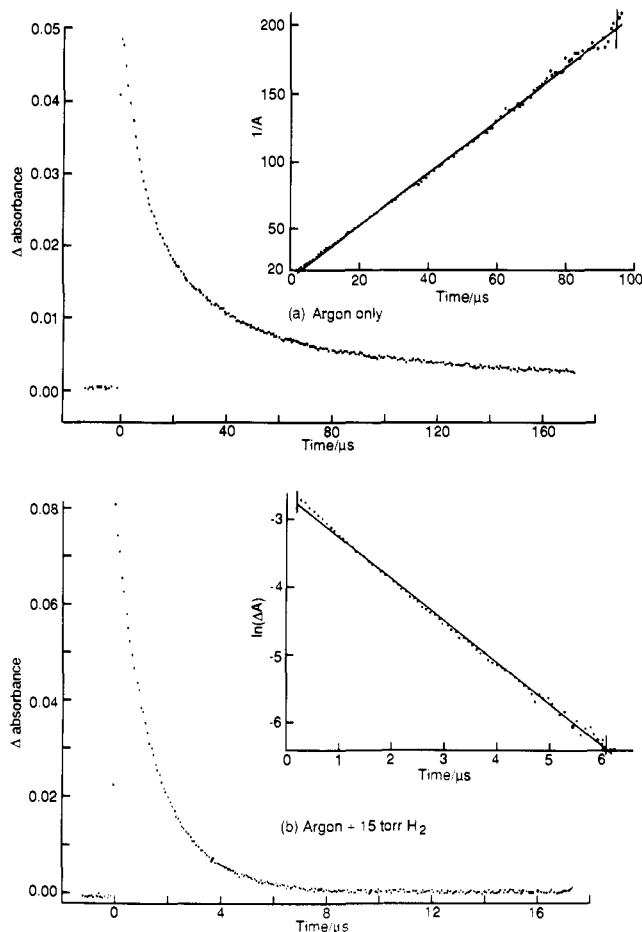


Figure 6. (a) Transient decay following laser flash photolysis (308 nm) of $\text{Ru}(\text{dmpe})_2\text{H}_2$ (ca. $4 \times 10^{-3} \text{ mol dm}^{-3}$) in cyclohexane solution under 1 atm of argon at 300 K monitored at 470 nm (average of 16 shots). Each dot represents an eight-point average of the output of the digital oscilloscope. The inset shows the second-order plot with the calculated line overlaying the experimental points and vertical bars on the plot to represent the limits used in the regression analysis. (b) Transient decay following laser flash photolysis of $\text{Ru}(\text{dmpe})_2\text{H}_2$ in cyclohexane under 15 Torr of H_2 made up to 1 atm with argon. The inset shows the first-order plot.

transient at 470 nm (Figure 8a); complete return back to the base line was no longer observed. The transient decayed with pseudo-first-order kinetics. A plot of k_{obsd} versus $[\text{CO}]$ showed that the decay was first order in $[\text{CO}]$, and (with the solubility of CO in cyclohexane taken as $9.3 \times 10^{-3} \text{ mol dm}^{-3} \text{ atm}^{-1}$)²² the second-order rate constant for the reaction with CO was calculated to be $(4.6 \pm 0.3) \times 10^9 \text{ dm}^3 \text{ mol}^{-1} \text{ s}^{-1}$ (Figure 7a).

Under 1 atm of CO, no transient could be detected at 470 nm, although the rapid rise (<100 ns) of a species absorbing at 365 nm could be detected. This product appeared to be stable for at least 100 ms.²³

The transient reacted similarly with ethene, but less rapidly than with CO. If the solubility of ethene is taken as $0.14 \text{ mol dm}^{-3} \text{ atm}^{-1}$,²² the second-order rate constant is determined as $(2.2$

(22) Wilhelm, E.; Bottino, R. *Chem. Rev.* **1973**, *73*, 1. There is no literature value for the solubility of ethene in cyclohexane. We have reduced the literature mole fraction of ethene in hexane by a factor of 0.65 corresponding to the ratio of the mole fractions of methane in cyclohexane and hexane, respectively.

(23) We have also used time-resolved infrared spectroscopy (TRIR) in cooperation with Dr. M. George and Prof. M. Poliakoff at the University of Nottingham to monitor the reaction with CO. Laser flash photolysis (308 nm) of $\text{Ru}(\text{dmpe})_2\text{H}_2$ (ca. $10^{-3} \text{ mol dm}^{-3}$) in *n*-heptane under 2 atm of CO results in the formation of a single product with $\nu(\text{CO})$ at 1857 cm^{-1} , which is assigned to $\text{Ru}(\text{dmpe})_2(\text{CO})$. The rise time of the product is within the resolution of the apparatus (ca. 400 ns). The depletion of the metal-hydride band at 1779 cm^{-1} could also be observed by TRIR, although the signal was too weak to be analyzed for any kinetics.

(21) Dymond, J. H. *J. Phys. Chem.* **1967**, *71*, 1829.

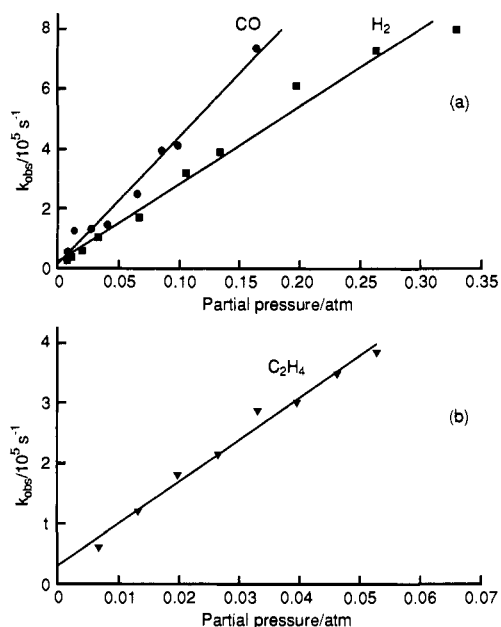


Figure 7. Plots of the pseudo-first-order rate constants for the decay of the transient obtained on laser flash photolysis of $\text{Ru}(\text{dmpe})_2\text{H}_2$ vs the partial pressure of added quenching gas for (a) H_2 (■), CO (●), and (b) C_2H_4 (▼). The best straight lines are shown as full lines through the experimental points.

Table IV. Second-Order Rate Constants for Reactions of $\text{Ru}(\text{dmpe})_2$ at 300 K

quencher	$k_2/\text{dm}^3 \text{ mol}^{-1} \text{ s}^{-1}$
H_2	$(6.2 \pm 0.3) \times 10^9$
CO	$(4.6 \pm 0.3) \times 10^9$
Me_3CNC	$(5.8 \pm 0.3) \times 10^8$
PMe_3	$(3.8 \pm 0.3) \times 10^8$
C_2H_4	$(2.2 \pm 0.4) \times 10^8$
Et_3SiH	$(2.1 \pm 0.2) \times 10^8$
cyclopentene	$(2.8 \pm 0.1) \times 10^7$

$\pm 0.4) \times 10^8 \text{ dm}^3 \text{ mol}^{-1} \text{ s}^{-1}$ (Figure 7b). As for the reaction with CO , the decay of the transient was too rapid to observe with 1 atm of ethene. However, the rapid rise ($<100 \text{ ns}$) of a product was monitored at 355 nm. The product was also detected in a UV/vis difference spectrum recorded after 200 laser shots.

d. Quenching by Cyclopentene, Triethylsilane, Trimethylphosphine and *tert*-Butyl Isocyanide. Addition of cyclopentene (10^{-2} – $10^{-1} \text{ mol dm}^{-3}$) to cyclohexane solutions of $\text{Ru}(\text{dmpe})_2\text{H}_2$ quenched the transient at 470 nm (Figure 8b), which decayed with pseudo-first-order kinetics (Figure 9a, Table IV). When the UV/vis spectrum of a solution containing $10^{-2} \text{ mol dm}^{-3}$ cyclopentene was examined after 200 laser shots, a broad maximum was found at 320 nm. When the cyclopentene concentration exceeded 0.4 mol dm^{-3} , the transient was too short-lived to be observed at 470 nm, but a product which was stable over at least $200 \mu\text{s}$ could be monitored at 360 nm.

Addition of triethylsilane (10^{-3} to $(2 \times 10^{-2}) \text{ mol dm}^{-3}$) to cyclohexane solutions of $\text{Ru}(\text{dmpe})_2\text{H}_2$ caused quenching of the transient at 470 nm. The transient decayed with pseudo-first-order kinetics, but the absorbance did not completely return to the base line. A plot of k_{obsd} vs $[\text{Et}_3\text{SiH}]$ shows a linear dependence on $[\text{Et}_3\text{SiH}]$ (Figure 9a, Table IV). The temperature dependence of the pseudo-first-order rate constant was measured over a range of 280–333 K with a concentration of triethylsilane of $1.7 \times 10^{-3} \text{ mol dm}^{-3}$. The activation parameters obtained were as follows: $E_a = 11.5 \pm 1.0 \text{ kJ mol}^{-1}$, $\Delta H^\ddagger = 8.9 \pm 1.0 \text{ kJ mol}^{-1}$, and $\Delta S^\ddagger = -53 \pm 4 \text{ J mol}^{-1} \text{ K}^{-1}$ (Figure 10).

Addition of trimethylphosphine ((5×10^{-4}) – $(3 \times 10^{-3}) \text{ mol dm}^{-3}$) resulted in quenching behavior similar to that observed with triethylsilane (Figure 9b, Table IV). Although the absorbance did not return to the base line, suggesting the presence of some longer lived photoproduct, we were unable to detect a photoproduct

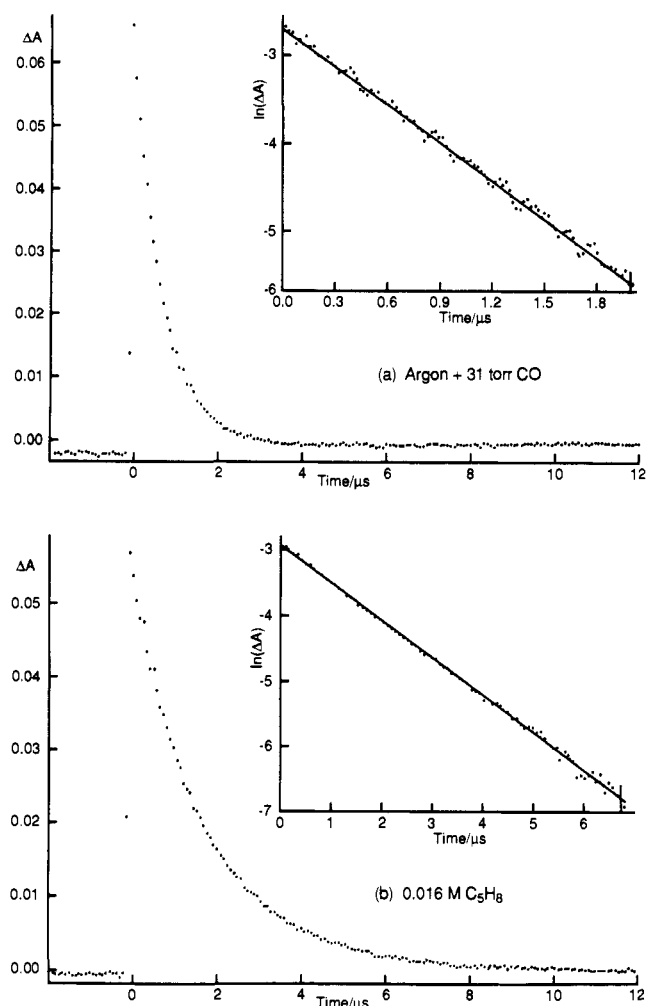


Figure 8. (a) Transient decay following laser flash photolysis of $\text{Ru}(\text{dmpe})_2\text{H}_2$ in cyclohexane solution under 31 Torr of CO made up to 1 atm with argon. The inset shows the corresponding first-order plot with two-point averaging instead of the usual eight-point average. (b) Transient decay and first-order plot from a similar experiment with $\text{Ru}(\text{dmpe})_2\text{H}_2$ in cyclohexane in the presence of $1.6 \times 10^{-2} \text{ mol dm}^{-3}$ cyclopentene.

from this reaction by NMR spectroscopy (see below). We therefore examined the transient over much longer time scales, but found no further decay up to 10 s.

Quenching by *tert*-butyl isocyanide ((6×10^{-5}) – $(8 \times 10^{-4}) \text{ mol dm}^{-3}$) was found to follow a similar pattern (Figure 9b, Table IV). The temperature dependence of the pseudo-first-order rate constant was measured over a temperature range 280–333 K with a concentration of Me_3CNC of $5.9 \times 10^{-5} \text{ mol dm}^{-3}$, yielding activation parameters as follows: $E_a = 4.9 \pm 0.6 \text{ kJ mol}^{-1}$, $\Delta H^\ddagger = 2.3 \pm 0.6 \text{ kJ mol}^{-1}$, and $\Delta S^\ddagger = -55 \pm 2 \text{ J mol}^{-1} \text{ K}^{-1}$.

3. Steady-State Photolysis Experiments with Carbon Monoxide, Ethene, Triethylsilane, and *tert*-Butyl Isocyanide. The reactions observed during flash photolysis experiments highlighted gaps in our knowledge of the ultimate photoproducts. Accordingly, we investigated the photolysis of $\text{Ru}(\text{dmpe})_2\text{H}_2$ with IR and NMR detection. $\text{Ru}(\text{dmpe})_2\text{H}_2$ was dissolved in isopentane and irradiated in a silica cuvette under 1 atm of CO for 1 min; a sample was then removed for IR spectroscopy. In addition to the Ru-H stretching band of the starting material at 1775 cm^{-1} , a sharp product band assigned to $\text{Ru}(\text{dmpe})_2\text{CO}$ was observed at 1858 cm^{-1} .

There appears to be a possible inconsistency between the literature results on the photochemical reaction of $\text{Ru}(\text{dmpe})_2\text{H}_2$ with ethene,⁷ claimed to give only an η^2 -complex, and those on reaction with cyclopentene,⁸ claimed to give only insertion products. Consequently, we reinvestigated the reaction with ethene. On photolysis of a methylcyclohexane-*d*₁₄ solution of

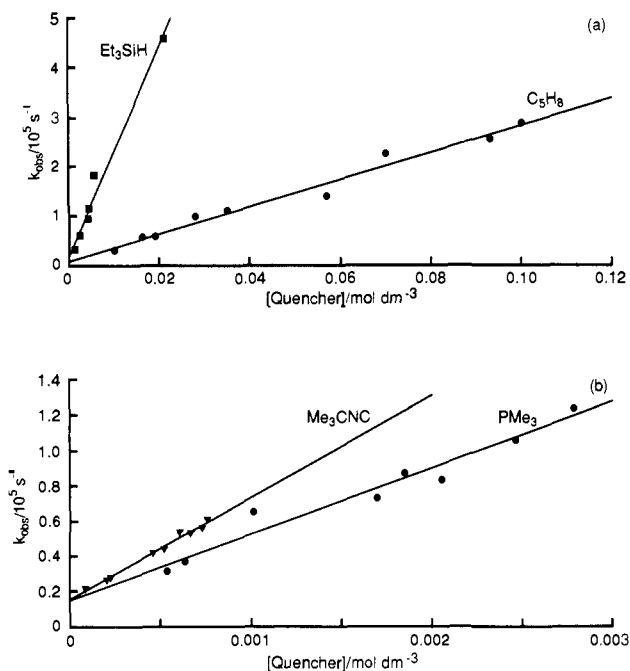


Figure 9. Plots of the pseudo-first-order rate constants for the decay of the transient obtained on laser flash photolysis of Ru(dmpe)₂H₂ vs the concentration of added quencher: (a) for triethylsilane (■) and cyclopentene (●) as quenchers; (b) for Me₃CNC (▼) and PMe₃ (●) as quenchers.

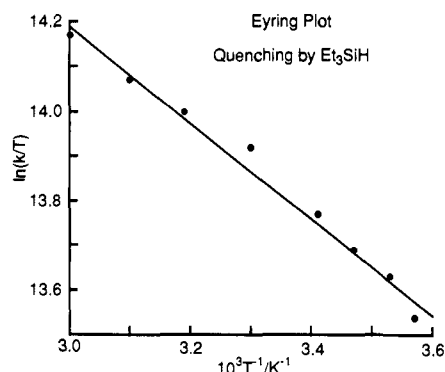


Figure 10. Eyring plot for the temperature dependence of the pseudo-first-order rate constant for reaction of the transient following laser flash photolysis of Ru(dmpe)₂H₂ in cyclohexane in the presence of triethylsilane ($1.7 \times 10^{-3} \text{ mol dm}^{-3}$); $\Delta H^\ddagger = 8.9 \pm 1.1 \text{ kJ mol}^{-1}$, $\Delta S^\ddagger = -53 \pm 4 \text{ J mol}^{-1} \text{ K}^{-1}$.

Ru(dmpe)₂H₂ under 1 atm of ethene at room temperature ($\lambda > 285 \text{ nm}$, 180 min), not only was Ru(dmpe)₂(C₂H₄) formed⁵ but a new metal hydride resonance also appeared at $\delta -8.52$ (dq, $J_{\text{PH}} = 87.6$ and 24.0 Hz) together with a series of new multiplets at $\delta 7.73$, 6.62 , and 5.88 (Figure 11). The resonances at $\delta 7.73$ and 5.88 both show large doublet couplings of 18.8 Hz , consistent with trans HH coupling across a double bond. The spectrum indicates that insertion into an ethene C–H bond has taken place to form the vinyl hydride complex, *cis*-Ru(dmpe)₂(C₂H₃)H. Unlike Fe(dmpe)₂(C₂H₃)H²⁴ and ($\eta^3\text{-C}_5\text{H}_5$)Rh(PMe₃)(C₂H₃)H,²⁵ Ru(dmpe)₂(C₂H₃)H is stable in solution at room temperature. The vinyl hydride complex may be formed directly from the starting material or by secondary photolysis of the ethene complex. Thus, the rapid quenching of Ru(dmpe)₂ under 1 atm of ethene in the flash photolysis experiment may represent a combination of η^2 -complexation and oxidative addition.

Although Tolman has reported the reaction of Fe(dmpe)₂(C₁₀H₇)H with Me₃SiH,²⁶ there are no reports in the literature

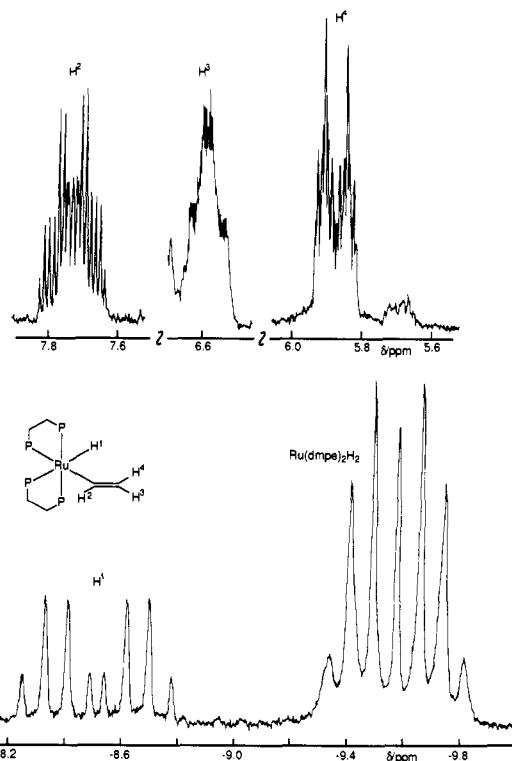


Figure 11. Partial ¹H NMR spectrum (300 MHz, C₆D₆) obtained following photolysis ($\lambda > 285 \text{ nm}$, 180 min) of Ru(dmpe)₂H₂ in methylcyclohexane in the presence of ethene showing the vinyl and the hydride resonances of Ru(dmpe)₂(C₂H₃)H. The higher field multiplet in the hydride region is due to the precursor.

for the reaction of Ru(dmpe)₂ with trialkylsilanes. Ru(dmpe)₂H₂ (ca. 15 mg) was photolyzed in neat Et₃SiH ($\lambda > 285 \text{ nm}$, 180 min) in an NMR tube at room temperature. The ¹H NMR spectrum recorded in cyclohexane-*d*₁₂ showed the presence of a triethylsilyl group ($\delta 1.32$, t, $J = 7.8 \text{ Hz}$ and $\delta 0.93$ m) and a new metal hydride at $\delta -9.74$. This resonance appeared as an apparent doublet of quartets ($J = 77$ and 25 Hz), although the pattern is very distorted. The ³¹P NMR spectrum ($\delta 35.9 \text{ m}$, 42.8 m) showed severe second-order effects. Although characterization of the product is incomplete, the spectra are consistent with 70% conversion to *cis*-Ru(dmpe)₂(SiEt₃)H.

The thermal reaction of Ru(dmpe)₂(naphthyl)H with isocyanides has been reported by Jones and Kosar.²⁷ Whereas reaction with Me₃CCH₂NC yields an isocyanide complex, a mixture of Ru(dmpe)₂(H)(CN) and Ru(dmpe)₂(CN)₂ is formed in the reaction with Me₃CNC. We examined the photochemical reaction of Ru(dmpe)₂H₂ with a 2-fold excess of Me₃CNC in hexane and observed the rapid formation of a white precipitate of Ru(dmpe)₂(CN)₂, identified by its ¹H NMR spectrum.²⁷ GC/MS revealed the formation of isobutane and several higher molecular mass organic products. No isobutene was detected, suggesting that any alkenes are immediately hydrogenated by Ru(dmpe)₂H₂.

We also examined the photochemical reaction of Ru(dmpe)₂H₂ with a 2-fold excess of PMe₃ in hexane, but found no products by ¹H or ³¹P NMR spectroscopy (recorded in C₆D₆).

Discussion

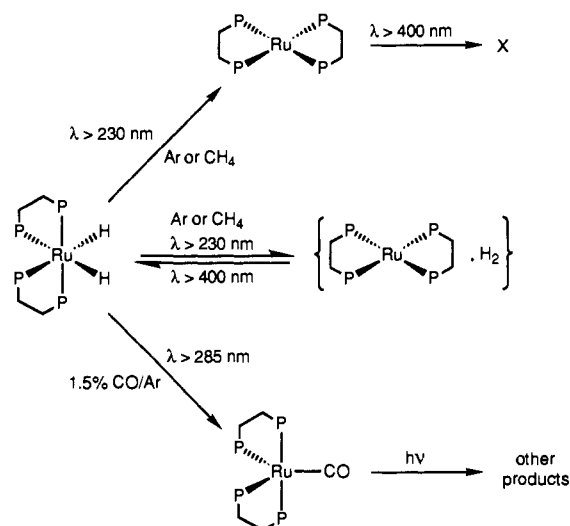
1. Identification of the Matrix Photoproduct. We have argued above that the irradiation of Ru(dmpe)₂H₂ in argon or methane matrices generates Ru(dmpe)₂ in two different environments denoted as P_{rev} and P_{irrev}. In P_{rev} the expelled dihydrogen lies close

(26) Tolman, C. A.; Ittel, S. D.; English, A. D.; Jesson, J. P. *J. Am. Chem. Soc.* **1978**, *100*, 7577.

(27) Jones, W. D.; Kosar, W. P. *Organometallics* **1986**, *5*, 1823. Examination of the ³¹P{¹H} spectrum of Ru(dmpe)₂(CN)₂ in CD₃CN showed two virtually coupled triplets at $\delta 33.6$ and $\delta 40.9$ ($J = 24 \text{ Hz}$). The chemical shifts in the above reference appear to have been recorded incorrectly.

(24) Baker, M. V.; Field, L. D. *J. Am. Chem. Soc.* **1986**, *108*, 7436.

(25) Bell, T. W.; Haddleton, D. M.; McCamley, A.; Partridge, M. G.; Perutz, R. N.; Willner, H. *J. Am. Chem. Soc.* **1990**, *112*, 9212.

Scheme I. Matrix Photochemistry of Ru(dmpe)₂H₂ at 12 K

to Ru(dmpe)₂, so that photochemical recombination to reform Ru(dmpe)₂H₂ occurs readily. In P_{irrev}, the dihydrogen has diffused out of reach and another photoprocess ensues. When the expelled dihydrogen is a close neighbor of the Ru(dmpe)₂, it perturbs the spectrum of the Ru(dmpe)₂. The mutual perturbation of the spectra of photoproducts trapped in the same matrix cage is long-established;²⁸ for instance, irradiation of Fe(CO)₅ generates Fe(CO)₄ and CO in two environments.^{28c} In one type the spectra of Fe(CO)₄ and the expelled CO are mutually perturbed and Fe(CO)₅ can be regenerated by near-IR radiation; in the other the spectra are unperturbed and the original reaction is irreversible. While the matrix isolation experiments (summarized in Scheme I) strongly suggest conversion of Ru(dmpe)₂H₂ to the 16-electron complex Ru(dmpe)₂ on photolysis, they are not conclusive until taken together with the laser flash photolysis experiments.

2. Identification of the Transient. The flash measurements made at room temperature yield a single intermediate which rises in <30 ns. Its spectrum bears a striking resemblance to the UV/vis spectra of the matrix photoproducts measured at 12 K (Figure 5), demonstrating that we are observing the same species. Moreover, this species must be in its ground state since the matrix is unable to trap an excited state. Its rapid rise confirms the conclusion of the matrix dilution experiments that it is a mononuclear species.

The kinetics of the decay of the transient also provides strong evidence for its identification as Ru(dmpe)₂. In alkane or arene solutions under an argon atmosphere, the decay of the intermediate is second order and the absorbance curve returns to the base line, indicating that back reaction with photoejected H₂ is the dominant reaction. The second-order kinetics can be readily understood since the concentrations of Ru(dmpe)₂ and H₂ are the same, so that we have a case of A + A kinetics.²⁹ The lack of dependence of the kinetics on the concentration of Ru(dmpe)₂H₂ (at constant cell path length) confirms that the decay does not involve reaction of the intermediate with the precursor. Further experiments at very high concentration in short path length cuvettes show that reaction with the precursor begins to be significant at ca. 2 × 10⁻² mol dm⁻³.

The transient is quenched by added hydrogen, with the consequence that it decays by pseudo-first-order kinetics. The resulting second-order rate constant in cyclohexane of 6.8 × 10⁹ dm³ mol⁻¹ s⁻¹ is close to the diffusion limit (according to Fick's first law, the diffusion-controlled rate in cyclohexane is 7.4 × 10⁹ dm³ mol⁻¹ s⁻¹). Since the slope of the plot of (absorbance)⁻¹ vs time without any added H₂ is k₂/εl and k₂ is known from the

quenching experiments, we may calculate the value of ε for the transient at 470 nm as ca. 2400 cm³ mol⁻¹ cm⁻¹ (see Table III). In the absence of added ligands or in the presence of hydrogen, the reaction is highly reversible.

The transient is quenched by a variety of other ligands, yielding new products. There is moderate selectivity for different reagents with variation in the rate constant of a factor of 240 (Table IV).

In conclusion, all of the kinetic evidence supports the identification of the transient as Ru(dmpe)₂. Further support comes from a consideration of the visible spectrum and from product identification. The transient solution photochemistry of Ru(dmpe)₂H₂ is summarized in Scheme II.

3. UV/Visible Spectrum of the Transient. The UV/vis spectra of square-planar d⁸ complexes have been the subject of extensive investigation. The spectra typically display low-energy bands with ε ≈ 800–15 000 dm³ mol⁻¹ cm⁻¹, which are much too intense for d-d transitions.^{30–34} Gray et al. assigned the lowest energy band for the complexes to the transition a_{1g}(d_{z²) → a_{2u}(p_z) in D_{4h} symmetry. The next transition to higher energy should then be e_g(d_{xz,yz}) → a_{2u}(p_z). In such a system, the a_{2u}(p_z) orbital is metal centered and nonbonding if the surrounding ligands are simple σ-bonding ligands. If suitable ligands are available, the orbital becomes π-bonding, so that d → p transitions become mixed with MLCT character. If the complex undergoes a D_{2d} distortion, the p_z orbital acquires b₂ symmetry and becomes σ-antibonding, implying that the d_{z² → p_z transition should move to higher energy. On the other hand, in D_{2h} symmetry, as appropriate to a planar chelate, the p_z orbital remains nonbonding suggesting that a very low-energy transition should be retained. However, the loss of degeneracy on moving from D_{4h} to D_{2h} may split other transitions.}}

The closest analogue of Ru(dmpe)₂ is the isoelectronic complex [Rh(dmpe)₂]⁺, which has a square-planar geometry.³⁵ The UV/vis spectrum of this complex in methanol³⁶ shows two clear bands at 309 and 390 nm of relative intensity 2:1. The related complex [Rh(PMe₃)₄]⁺ show only one band at 470 nm in acetonitrile solution.³⁷ However, the crystal structure of this complex shows substantial puckering which distorts the geometry toward tetrahedral.³⁸

The spectrum of Ru(dmpe)₂ is red-shifted by as much as 12 000 cm⁻¹ compared to [Rh(dmpe)₂]⁺, probably because of the reduction in charge. The extremely low energy of the first transition, which is a common feature in the spectra of other square-planar complexes, suggests that Ru(dmpe)₂ is itself square planar. Assignments for the absorption bands made on this basis are given in Table III.

The shifts between the UV/vis maxima of Ru(dmpe)₂ in the two matrix forms and between different matrices are in the range 70–700 cm⁻¹ and are far too small to support any specific interaction with dihydrogen or methane as observed for Cr(CO)₅.³⁹ The biggest difference between the band positions of P_{irrev} and those of Ru(dmpe)₂ in cyclohexane is ca. 1550 cm⁻¹.

4. Identification of Final Products and Comparative Kinetics. The transient, Ru(dmpe)₂, reacts with hydrogen at a rate which is close to diffusion-controlled. The kinetic isotope effect observed for addition of H₂ and D₂ to Ru(dmpe)₂ (k_H/k_D ≈ 1.3) is consistent with data in the literature^{40,41} and suggests that very little

(30) Geoffroy, G. L.; Wrighton, M. S.; Hammond, G. S.; Gray, H. B. *J. Am. Chem. Soc.* **1974**, *96*, 3105.

(31) Lever, A. B. P. *Inorganic Electronic Spectroscopy*, 2nd ed.; Elsevier: Amsterdam, 1984.

(32) Smith, D. C.; Miskowski, V. M.; Mason, W. R.; Gray, H. B. *J. Am. Chem. Soc.* **1990**, *112*, 3759.

(33) Andrews, L. *J. Inorg. Chem.* **1978**, *17*, 3180.

(34) Fordyce, W. A.; Crosby, G. A. *Inorg. Chem.* **1982**, *21*, 1455.

(35) Marder, T. B.; Williams, I. D. *J. Chem. Soc., Chem. Commun.* **1987**, 1478.

(36) [Rh(dmpe)₂]Cl was synthesized by the method of Butter and Chatt (Butter, S. A.; Chatt, J. *J. Chem. Soc. A* **1970**, 1411) and characterized by ³¹P NMR spectroscopy as in ref 35.

(37) Jones, W. D. Unpublished observations.

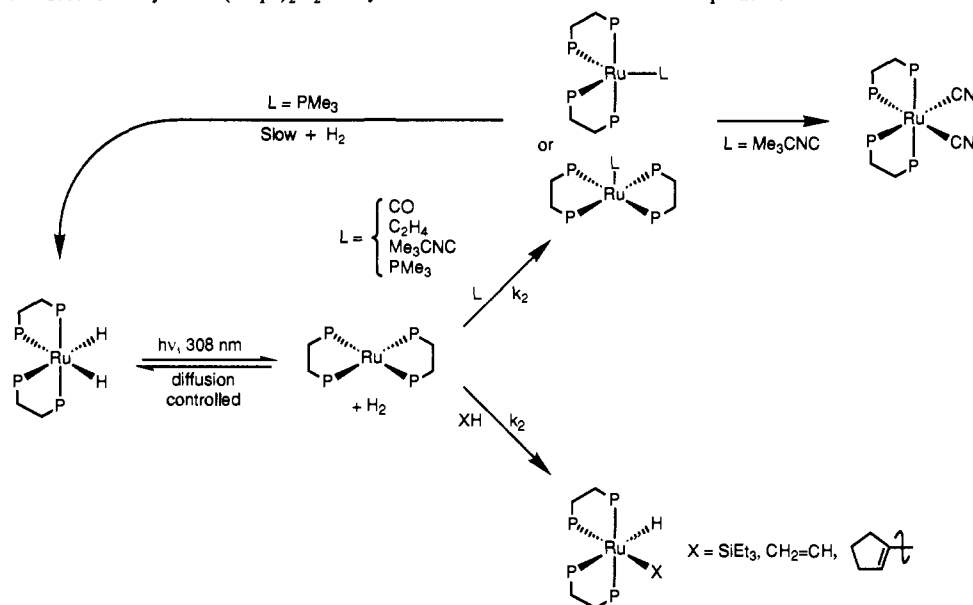
(38) Jones, R. A.; Real, F. M.; Wilkinson, G.; Galas, A. M. R.; Hursthouse, M. B. *J. Chem. Soc., Dalton Trans.* **1980**, 511.

(39) Perutz, R. N.; Turner, J. J. *J. Am. Chem. Soc.* **1975**, *97*, 4791.

(40) Wasserman, E. P.; Moore, C. B.; Bergman, R. G. *Science* **1992**, *255*, 315. (b) Wink, D. A.; Ford, P. C. *J. Am. Chem. Soc.* **1987**, *109*, 436.

(28) (a) Perutz, R. N. *Chem. Rev.* **1985**, *85*, 97. (b) Clemitshaw, K. C.; Sodeau, J. *J. Phys. Chem.* **1988**, *92*, 5491. (c) Poliakoff, M.; Turner, J. J. *J. Chem. Soc., Dalton Trans.* **1973**, 1351.

(29) Moore, J. W.; Pearson, R. G. *Kinetics and Mechanism*, 3rd ed.; Wiley: New York, 1981.

Scheme II. Transient Photochemistry of Ru(dmpe)₂H₂ in Cyclohexane Solution at Ambient Temperature

H-H bond breaking takes place in the approach to the transition state. This deduction is compatible with either a smooth reaction (with no intermediate) or a reaction proceeding via an η^2 -H₂ intermediate. However, we prefer the former interpretation since we would have to assume in the latter case that the η^2 -H₂ intermediate is undetectable by UV/vis spectroscopy. It is remarkable that the reaction with H₂ is so rapid, considering the change in geometry from square-planar Ru(dmpe)₂ to *cis*-Ru(dmpe)₂H₂.

There are no examples in the literature of rate constants for reaction with hydrogen in solution that are as large as 10⁹ dm³ mol⁻¹ s⁻¹. Very recently, however, Wasserman et al. reported that reaction of (η^5 -C₅H₅)RhCO with H₂ in the gas phase occurs on every collision.^{40a} In contrast, the rate constant for reaction of tricoordinate RhCl(PPh₃)₂ with H₂ in solution is 10⁵ dm³ mol⁻¹ s⁻¹.^{40b} In other cases, hydrogen is coordinated as an intact η^2 -H₂ complex.⁴² W(CO)₃(PCy₃)₂ (Cy = cyclohexyl) reacts with H₂ to form W(CO)₃(PCy₃)₂(η^2 -H₂), with a rate constant of 2.2 × 10⁶ dm³ mol⁻¹ s⁻¹.⁴¹

The approach of H₂ to a square-planar d⁸ system has been investigated by extended Hückel calculations.^{43,44} When H₂ approaches either perpendicular or parallel to the plane of the organometallic fragment, the total computed energy curve is repulsive. However, if one pair of mutually trans ligands is bent back to give a C_{2v} fragment, oxidative addition is favored.

Decay of the transient in the presence of CO as a quenching ligand is also close to diffusion-controlled. The product, Ru(dmpe)₂(CO), may be identified from the IR spectra obtained in CO-doped matrices, in static solution experiments, and in time-resolved IR experiments.²³ Ru(dmpe)₂(CO) has been shown crystallographically to possess a trigonal-bipyramidal structure in which the CO occupies an equatorial site.¹⁹ Thus, the extremely rapid reaction with CO, as with H₂, implies that there is a minimal barrier to rearrangement of the RuP₄ skeleton.

Rates of reaction with CO have been used extensively to probe the structure of organometallic reaction intermediates.⁴⁵⁻⁴⁹ The

rate constant for the reaction of Fe(CO)₄ with CO is about 700 times slower than that of Cr(CO)₅ with CO because Fe(CO)₄ is a triplet whereas Cr(CO)₅ is a singlet.^{48,49} On the other hand, TRIR measurements indicate that Ru(CO)₄ and Os(CO)₄ have singlet ground states.^{16,50} The large rate constant for reaction of Ru(dmpe)₂ with CO in solution (ca. 5 × 10⁹ dm³ mol⁻¹ s⁻¹) implies that Ru(dmpe)₂ has a singlet ground state.

A direct comparison of the reactivity of another unsaturated fragment with H₂ and CO is possible for several coordinatively unsaturated molecules. RhCl(PPh₃)₂ reacts with CO about 700 times faster than with H₂.^{40b} Hoff et al., who observed a similar phenomenon with W(CO)₃(PCy₃)₂, have proposed that the slower reaction with hydrogen arises from the barrier to breaking the H-H bond of the molecular hydrogen complex rather than any barrier in the binding to molecular hydrogen.⁴¹ Evidently, this is not the case for Ru(dmpe)₂, (η^5 -C₅H₅)RhCO, and Fe(CO)₄, where the rates of reaction with H₂, D₂, and CO are similar.^{40a,49c}

The reactions between Ru(dmpe)₂ and unsaturated organic ligands are somewhat more puzzling. On flash photolysis of Ru(dmpe)₂H₂ in benzene solution only back reaction with H₂ is observed, although prolonged static photolysis does yield the phenyl hydride complex.⁸ The lack of solvent activation in the flash experiments would appear to indicate that H₂ readdition to Ru(dmpe)₂ is able to compete very effectively with benzene addition, even though the concentration of hydrogen is very low.

In contrast, cyclopentene quenches Ru(dmpe)₂ at low concentrations of added ligand, although alkenic C-H bond activation proceeds at a rate similar to benzene activation in static photolysis experiments.⁸ This observation suggests that we may be detecting the metal alkene complex rather than the cyclopentenyl hydride under the flash conditions. The cyclopentenyl hydride complex may be formed in a slower competing pathway or by secondary photolysis of the cyclopentene complex.²⁵ The reaction with ethene raises similar problems.

The reaction of Ru(dmpe)₂ with Et₃SiH is shown by NMR to yield *cis*-Ru(dmpe)₂(SiEt₃)H. This is an unambiguous case of oxidative addition, with a second-order rate constant of ca. 2 × 10⁸ dm³ mol⁻¹ s⁻¹ and an enthalpy of activation of only 8.9 kJ

(41) Zhang, K.; Gonzalez, A. A.; Hoff, C. D. *J. Am. Chem. Soc.* **1989**, *111*, 3627.

(42) (a) Church, S. P.; Grevels, F.-W.; Hermann, H.; Schaffner, K. *J. Chem. Soc., Chem. Commun.* **1985**, 30. (b) Sweany, R. L. *J. Am. Chem. Soc.* **1985**, *107*, 2374.

(43) Dedieu, A.; Strich, A. *Inorg. Chem.* **1979**, *18*, 2940.

(44) Saillard, J.-Y.; Hoffmann, R. *J. Am. Chem. Soc.* **1984**, *106*, 2006.

(45) Weitz, E. *J. Phys. Chem.* **1987**, *91*, 3945.

(46) Creaven, B. S.; Dixon, A. J.; Kelly, J. M.; Long, C.; Poliakoff, M. *Organometallics* **1987**, *6*, 2600.

(47) (a) Bonneau, R.; Kelly, J. M. *J. Am. Chem. Soc.* **1980**, *102*, 1220. (b) Kelly, J. M.; Long, C.; Bonneau, R. *J. Phys. Chem.* **1983**, *87*, 3344.

(48) (a) Seder, T. A.; Church, S. P.; Ouderkirk, A. J.; Weitz, E. *J. Am. Chem. Soc.* **1985**, *107*, 1432. (b) Seder, T. A.; Church, S. P.; Weitz, E. *J. Am. Chem. Soc.* **1986**, *108*, 4721. (c) Fletcher, T. R.; Rosenfeld, R. N. *J. Am. Chem. Soc.* **1983**, *105*, 6358. (d) Fletcher, T. R.; Rosenfeld, R. N. *J. Am. Chem. Soc.* **1985**, *107*, 2203.

(49) (a) Ouderkirk, A. J.; Weitz, E. *J. Chem. Phys.* **1983**, *79*, 1089. (b) Seder, T. A.; Ouderkirk, A. J.; Weitz, E. *J. Chem. Phys.* **1986**, *85*, 1977. (c) Ryther, R. J.; Weitz, E. *J. Phys. Chem.* **1991**, *95*, 9841. Note that data for the reaction of Fe(CO)₄ with D₂ are not available.

(50) Bogdan, P. L.; Weitz, E. *J. Am. Chem. Soc.* **1990**, *112*, 639.

mol^{-1} . The entropy of activation is negative, as expected.

The reaction with PMe_3 is assumed to generate $\text{Ru}(\text{dmpe})_2(\text{PMe}_3)$, which has been synthesized previously by a thermal route.¹⁹ However, the product appears unstable with respect to reaction with H_2 to regenerate $\text{Ru}(\text{dmpe})_2\text{H}_2$. The reaction with Me_3CNC generates $\text{Ru}(\text{dmpe})_2(\text{CN})_2$, presumably via $\text{Ru}(\text{dmpe})_2(\text{CNCMe}_3)$. The latter would be analogous to the $\text{CNCH}_2\text{CMe}_3$ derivative which has been formed thermally.²⁷ The susceptibility of the *tert*-butyl derivative to elimination has been contrasted with the behavior of the *tert*-butylmethyl complex.²⁷

There is no evidence that $\text{Ru}(\text{dmpe})_2$ reacts or interacts appreciably with alkanes either in solution or in methane matrices. The perturbation of the electronic spectrum by expelled dihydrogen or by the matrix is too small to involve a specific interaction with the metal center. Saillard and Hoffmann have shown that the approach of CH_4 (both parallel and perpendicular) to square-planar and angular $d^8 \text{ML}_4$ fragments is repulsive.⁴⁴ The parallel approach which is so favored for hydrogen is now dominated by steric repulsion; our findings are consistent with this behavior.

Conclusions

1. The combination of low-temperature matrix, solution flash photolysis, and static solution photolysis of $\text{Ru}(\text{dmpe})_2\text{H}_2$ provides compelling evidence for the formation of $\text{Ru}(\text{dmpe})_2$ in the primary photochemical event. The rise time of $\text{Ru}(\text{dmpe})_2$ is demonstrated by the current experiments to be $<30 \text{ ns}$.⁵¹

2. $\text{Ru}(\text{dmpe})_2$ probably has a square-planar structure with no specific interaction with dihydrogen or methane. It is generated in two forms in matrices. In one, the expelled hydrogen is close to $\text{Ru}(\text{dmpe})_2$ and selective irradiation regenerates $\text{Ru}(\text{dmpe})_2\text{H}_2$. In the other form, dihydrogen has diffused too far for recombination.

3. In the absence of other ligands, $\text{Ru}(\text{dmpe})_2$ decays in solution by reaction with photoejected H_2 to regenerate $\text{Ru}(\text{dmpe})_2\text{H}_2$.

4. Reaction with added H_2 or CO is near diffusion-controlled, implying that $\text{Ru}(\text{dmpe})_2$ is a singlet. The rapid back reaction with H_2 reduces the utility of the dihydride as a precursor to a C-H activating fragment.

5. $\text{Ru}(\text{dmpe})_2$ shows a high reactivity toward cyclopentene, Et_3SiH , ethene, PMe_3 , and Me_3CNC . NMR studies have shown that $\text{Ru}(\text{dmpe})_2$ reacts photochemically with ethene to give both $\text{Ru}(\text{dmpe})_2(\text{C}_2\text{H}_4)$ and $\text{Ru}(\text{dmpe})_2(\text{C}_2\text{H}_5)\text{H}$.

6. The reactivity and spectra of $\text{Ru}(\text{dmpe})_2$ contrast sharply with those of $\text{Fe}(\text{dmpe})_2$.⁵² On the other hand, $\text{Ru}(\text{dmpe})_2$ bears a considerable resemblance to $\text{Ru}(\text{CO})_2(\text{PMe}_3)_2$ spectroscopically.⁵²

Experimental Section

Materials. Ruthenium trichloride, dmpe , Me_3CNC , and PMe_3 were purchased from Aldrich. Deuterated solvents were obtained from Goss Scientific or MSD Isotopes. Gases for synthesis were of commercial grade, whereas those for matrix isolation and flash photolysis experiments were of research grade (B.O.C.). Deuterium was obtained from B.O.C. (research grade 99.7% D). Solvents for synthesis (AR grade) were dried by refluxing over sodium benzophenone ketyl under an argon atmosphere, while those for flash photolysis (Aldrich HPLC grade) were dried over CaH_2 under argon. Cyclopentene (Fluka, puriss. >99.5%) and triethylsilane (Fluka, >99%) were distilled under a nitrogen atmosphere and stored over grade 3A molecular sieves.

Synthesis of *cis*- $\text{Ru}(\text{dmpe})_2\text{H}_2$. Syntheses were carried out on standard Schlenk lines under an argon atmosphere. *trans*- $\text{Ru}(\text{dmpe})_2\text{Cl}_2$ was synthesized and converted to *cis*- $\text{Ru}(\text{dmpe})_2(\text{naphthyl})\text{H}$ following the literature methods with minor modifications.² A solution of *cis*- $\text{Ru}(\text{dmpe})_2(\text{naphthyl})\text{H}$ in toluene (10 cm^3) was heated in an ampule under 1 atm of hydrogen at 80°C for 24 h. The solution was left to cool and then placed under fresh hydrogen and heated at 80°C for an additional 24 h. The solvent was removed in vacuo leaving an orange oil, which was

sublimed at 60°C onto a water-cooled finger to yield colorless needles of *cis*- $\text{Ru}(\text{dmpe})_2\text{H}_2$. The purity was checked by comparison of the ^1H and ^{31}P NMR spectra with the published data.⁵ *cis*- $\text{Ru}(\text{dmpe})_2\text{D}_2$ was prepared in a similar manner with deuterium used in place of hydrogen.

Matrix Isolation Methods. The matrix isolation apparatus is described in detail elsewhere.³³ Samples for IR spectroscopy alone were deposited onto a CsI window cooled by an Air Products CS202 closed-cycle refrigerator to 12–25 K. A BaF_2 window was used for combined IR and UV/vis spectroscopy. The outer windows of the vacuum shroud were chosen to match. *cis*- $\text{Ru}(\text{dmpe})_2\text{H}_2$ was sublimed from a right-angled glass tube heated to 330–338 K at the same time as a gas stream entered the vacuum shroud through a separate inlet. Typical deposition temperatures and rates were 20 K for Ar (2 mmol h^{-1}) and 25 K for CH_4 (2 mmol h^{-1}). The samples were then cooled to 12 K before recording IR spectra on a Mattson Sirius FTIR spectrometer fitted with a TGS detector and KBr beam splitter, which was continuously purged with dry CO_2 -free air. Spectra were recorded at 1 cm^{-1} resolution with 128 scans coaveraged (25K data points with two times zero-filling). UV/vis spectra were recorded on the same sample at the same temperature on a Perkin-Elmer Lambda 7G spectrometer. Matrices were photolyzed through a quartz window with a Philips HPK 125-W medium-pressure mercury arc, quartz focusing lens, and water filter or with an ILC 302UV 300-W Xe arc equipped either with UV-reflecting (240–400 nm) or with visible-reflecting (400–800 nm) mirrors and a water filter. Photolysis wavelengths were selected with cutoff or interference filters or a Schott UG11 filter (234–376 nm).

Laser Flash Photolysis. The apparatus for laser flash photolysis has been described previously.⁵⁴ In brief, a XeCl laser (308 nm, 30 ns pulse width, 40 mJ pulse^{-1}) is used as the exciting source and a pulsed Xe arc acts as the monitoring source. The Applied Photophysics spectrometer is linked to a Gould 4500 digital oscilloscope. The rise time of the apparatus is 50–100 ns. Since publication of the earlier description, the beam path has been modified with the aid of two dichroic mirrors (Technical Optics) which reflect 308-nm radiation when set at 45° to the incident beam. The laser beam now travels through the sample at 180° to the monitoring beam. The laser is operated at a 1 Hz repetition rate and focused to a 5 mm diameter spot at the sample. Signals are usually detected by an IP28 photomultiplier, but this was replaced by an R928 tube in order to make measurements out to 800 nm. Transient signals were usually collected as 16-shot averages on the digital oscilloscope before transfer to the Apple II microcomputer (via a Biodata Microlink III), which also served to control the timing of the laser, arc lamp, and shutters. The 2000 data points were reduced to 250 as 8-, 4-, or 2-point averages of the first 2000, 1000, or 500 points according to the time span of interest. The minimum data point interval is 10 ns. Decays were analyzed by linear least-squares regression methods after conversion to absorbance. Error bars are quoted as 95% confidence limits. In recent experiments, the Apple computer and Microlink were replaced by a Dell PC with dedicated timing-board and in-house software. All 2000 data points were then analyzed without averaging.

Transient spectra were also recorded on a very similar apparatus in Ottawa which incorporated a Lumonics excimer laser (308 nm, 5 ns pulse width, 30 mJ pulse^{-1}), a 150-W arc as monitoring source, a CVI Digi-krom monochromator, an RCA 8480 (or R928) photomultiplier tube, a Tektronix 2440 digital oscilloscope, and a Mackintosh IICI computer with National Instruments interfaces and Labview software. This apparatus was designed with the excitation beam at 90° to the monitoring beam. More details of this equipment will be published elsewhere. Although the wavelengths of the band maxima measured in Ottawa agreed with measurements in York, their relative intensities showed variation outside experimental error. Checks of the photometric accuracy of both the York and Ottawa instruments failed to reveal any systematic errors. We attribute the variation in the transient spectra to differences in photomultiplier performance. The spectra illustrated in Figure 5 and the relative intensities of Table III are taken from spectra measured in Ottawa.

Samples for flash experiments were sublimed immediately before use and loaded in a glove box into a quartz cuvette (1, 2, or 10 mm path length) fitted with a PTFE stopcock and degassing bulb. Solvent was added via a cannula on a Schlenk line evacuated by a diffusion pump to 10^{-4} mbar and filled with argon. The sample was degassed by three freeze-pump-thaw cycles (10^{-4} mbar) before back-filling to 1 atm with the appropriate gas. Gas mixtures were made up manometrically to 1 atm in 1-L bulbs, so that the pressure in the flash cell was typically 700 Torr. Solutions with liquid quenchers were made up either by addition

(51) We have already made preliminary measurements on the picosecond time scale which indicate that the rise time may be as low as 16 ps: Osman, R.; Perutz, R. N.; Rooney, A. D. Unpublished observations. Quantum yields and bond enthalpies determined by photoacoustic spectroscopy will be reported separately. Belt, S. T.; Scaiano, J. C.; Whittlesey, M. K. *J. Am. Chem. Soc.*, submitted for publication.

(52) Whittlesey, M. K. D. Phil. Thesis, University of York, York, UK, 1991.

(53) Haddleton, D. M.; McCamley, A.; Perutz, R. N. *J. Am. Chem. Soc.* **1988**, *110*, 1810.

(54) Belt, S. T.; Grevels, F.-W.; Klotzbücher, W.; McCamley, A.; Perutz, R. N. *J. Am. Chem. Soc.* **1989**, *111*, 8373.

of quencher to the cuvette with a microliter syringe (Et_3SiH , cyclopentene) or by employing stock solutions (PMe_3 , tBuNC). In the latter case, a measured quantity of gas was condensed into a measured volume of cyclohexane on a high-vacuum line. The absorbances of the solutions for flash photolysis experiments were in the range 0.5–1.0 at 308 nm. Variable-temperature measurements were made by replacing the standard sample holder by an insulated holder mounted on a block through which thermostated water was circulated.

Steady-State Photolysis. Steady-state photolysis experiments were usually performed in NMR tubes in situ. NMR spectra were recorded on a Bruker MSL 300-MHz spectrometer. ^1H spectra were referenced to solvent peaks as follows: $\text{C}_6\text{D}_5\text{H}$ δ 7.13, cyclohexane- d_{11} δ 1.38, me-

thylcyclohexane- d_{13} δ 1.36. ^{31}P spectra were referenced relative to 85% H_3PO_4 at $\delta = 0$.

Acknowledgment. We are grateful to Dr. O. Traverso and Dr. L. D. Field for helpful discussions and for disclosing data prior to publication, to Dr. S. E. J. Bell for advice on optics, to D. Dukic for his work in interfacing and development of software, and to Prof. M. Poliakoff and Dr. M. George for carrying out the time-resolved IR experiment. We acknowledge the support of The Fulbright Commission, The Royal Society, SERC, NATO, British Gas, and the EC Commission.

Trifluoroacetic Acid Tetrahydrate: A Unique Change from an Ionic to a Molecular Crystal Structure on Deuteration¹⁻³

Dietrich Mootz* and Michaela Schilling

Contribution from the Institut für Anorganische Chemie und Strukturchemie, Heinrich-Heine-Universität Düsseldorf, D-4000 Düsseldorf, Federal Republic of Germany. Received December 3, 1991

Abstract: Trifluoroacetic acid has been found from DTA, DSC, and temperature-dependent X-ray powder diffraction to form, besides other stable and metastable hydrates, both an undeuterated (reinvestigation) and perdeuterated stable tetrahydrate. For the undeuterated phase (mp -12°C) an ionic structure, $(\text{H}_5\text{O}_2)[(\text{CF}_3\text{COO})_2\text{H}]\cdot 6\text{H}_2\text{O}$, has been confirmed by X-ray analysis. In contrast, the perdeuterated tetrahydrate (mp -15°C) has been found to be molecular, i.e. with $\text{CF}_3\text{COOD}\cdot 4\text{D}_2\text{O}$ not only as the empirical but also as the pertinent structural formula. This unprecedented effect of a deuteration is distinct and unmistakable, since there are specific and consistent differences of position not only for certain H and D atoms but also for crucial heavier atoms. In other ways the two structures are strikingly similar, with three of the four water molecules hydrogen-bonded in characteristic layers of identical topologies.

Trifluoroacetic acid, due to the profound ($-I$) effect of the three fluorine atoms on the α -carbon atom, is a carboxylic acid of outstanding strength. The dissociation constant, according to the most recent determination by Raman spectroscopy, is $K = 0.66 \pm 0.25$ mol/L.⁴ It is therefore surprising that, by crystal structure analysis of the two hydrates of the acid, only the tetrahydrate, as $(\text{H}_5\text{O}_2)[(\text{CF}_3\text{COO})_2\text{H}]\cdot 6\text{H}_2\text{O}$, was found to be ionic, while the monohydrate, as $\text{CF}_3\text{COOH}\cdot\text{H}_2\text{O}$, was found to be molecular.⁵ This exceptional 2-fold behavior of an acid as a lower and a higher crystalline hydrate raised the question as to its possible susceptibility to hydrogen/deuterium substitution. Hence it was decided to perform a combined phase and structural analysis on the perdeuterated system of the acid and water as well and, in order to achieve an optimal comparison with the undeuterated one, to reexamine most results for the latter.⁵

Results

Phase Relations. The melting diagram of the undeuterated and perdeuterated (quasi)binary acid-water system, as obtained by DTA and DSC as well as temperature-dependent X-ray powder diffraction, is depicted in Figure 1. The diagrams show the existence of both an undeuterated and perdeuterated mono- and tetrahydrate, each of which melts congruently at reduced temperatures. The perdeuterated tetrahydrate forms a low- and a

Table I. Undeuterated and Perdeuterated Stable and Metastable Phases of Crystalline Hydrates of Trifluoroacetic Acid

monohydrate mp -39°C	} isotypic	monohydrate metastable	} isotypic
monohydrate- d_3 mp -36°C		monohydrate- d_3 metastable	
tetrahydrate ^a mp -12°C	} isotypic	tetrahydrate metastable	} isotypic
tetrahydrate- d_9 low-temp form stable up to -43°C		tetrahydrate- d_9 metastable, no. 1	
tetrahydrate- d_9 high-temp form ^a mp -15°C		tetrahydrate- d_9 metastable, no. 2	

^a The crystal structures of these two phases are dealt with in this paper.

high-temperature phase. The pertinent transition temperature and all melting points are compiled in Table I, along with additional, metastable phases detected and indications of structural isotype correspondence.

Most of the metastable phases were observed as primary products of crystallization from a glassy state, formed by quenching liquid samples down to the temperature of liquid nitrogen. The second metastable phase of the perdeuterated tetrahydrate was obtained directly from the melt; the undeuterated metastable tetrahydrate was obtained in both ways.

As for the stable phases and in view of the two crystal structures to be dealt with in detail in the following, particular attention is drawn to the fact that the undeuterated tetrahydrate is isotypic with the low-temperature perdeuterated one, while the high-temperature counterpart of the latter has a unique structure.

(1) Dedicated to Professor Alois Haas on the occasion of his 60th birthday.

(2) This is paper 30 of our series Fluorides and Fluoro Acids and paper 34 of our series Crystal Structures of Acid Hydrates and Oxonium Salts. For papers 29 and 33 see: Mootz, D.; Bartmann, K. *Z. Naturforsch.* 1991, 46B, 1659-1663. Mootz, D.; Bartmann, K. *Z. Anorg. Allg. Chem.* 1991, 592, 171-178.

(3) Schilling, M. Dissertation in progress Universität Düsseldorf.

(4) Strehlow, H.; Hildebrandt, P. *Ber. Bunsen-Ges. Phys. Chem.* 1990, 94, 173-179.

(5) Mootz, D.; Boenigk, D. *Z. Naturforsch.* 1984, 39B, 298-304.